and A. Keller, *ibid.*, 11, 193 (1973).
(3) J. I. Lauritzen, Jr., and J. D. Hoffman, *J. Appl. Phys.*, **44**, 4340 (1973).
(4) F. C. Frank and M. Tosi, *Proc. R. Soc. London, Ser. A*, **263**, 323 (1960).
(5) J. D. Hoffman, G. T. Davis, and J. I. Lauritzen, Jr., "Treatise on Solid State Chemistry", Vol. 3, N. B. Hannay Ed., Plenum Press, New York, 1976, Chapter 7.
(6) M. Abramowitz and I. A. Stegun, "Handbook of Mathematical Functions", Dover Publications, New York, 1965, pp 310–316.
(7) R. L. Miller, *Kolloid Z. Z. Polym.*, **225**, 62 (1968).
(8) M. Dupire et al., to be published.
(9) B. Wunderlich, "Macromolecular Physics", Vol. 2, Academic Press, New York, 1976.
(10) D. Turnbull and J. C. Fisher, *J. Chem. Phys.*, **17**, 71 (1949).
(11) J. D. Hoffman, G. S. Ross, L. Frolen, and J. I. Lauritzen, *J. Res. Natl. Bur. Stand., Sect. A*, **79**, 671 (1975).
(12) J. J. Labaig, Ph.D. Thesis, Fac. Sciences, Strasbourg, 1978.
(13) D. M. Sadler and A. Keller, *Macromolecules*, **10**, 1128 (1977).
(14) A. J. Kovacs, C. Straupe, and A. Gonthier, *J. Polym. Sci., Polym. Symp.*, **59**, 31 (1977).
(15) P. Dreyfuss and A. Keller, *J. Macromol. Sci., Phys.*, **4**, 811 (1970).
(16) J. J. Point and A. Goffin, *J. Polym. Sci., Polym. Lett. Ed.*, **13**, 249 (1975).
(17) If n_i', n_i'', and n_i''' denote the occupation numbers for nuclei of length $i\Delta l$, made of 2, 3, ... stems, their rates of change are given by $dn_i/dt = An_{i-1} - (A + B + C_{i+})n_i + Bn_{i+1} + C_{i-}n_i'$, $dn_i'/dt = C_{i+}n_i - (C_{i+} + C_{i-})n_i' + C_{i-}n_i''$, and $dn_i''/dt = ...$, where C_{i+} and C_{i-} denote the rate constant for folding and unfolding, respectively. In the steady state, we obtain, under the assumption $C_{i+} > C_{i-}$, $n_i = n_i' = n_i'' = n_i'''$ and eq 1, where $C_i = C_{i+} - C_{i-}$.

Carbon-13 Magnetic Relaxation Study of the Internal Motions of Poly(4-vinyl-*N*-*n*-alkylpyridinium bromides) in Methanol Solutions

Denis Ghesquiere and Claude Chachaty*

Service de Chimie Physique, Centre d'Etudes Nucléaires de Saclay, 91190 Gif-sur-Yvette, France

Akihiro Tsutsumi

Department of Polymer Science, Faculty of Sciences, Hokkaido University, Sapporo 060, Japan. *Received January 4, 1979*

ABSTRACT: The dynamical behavior of poly(4-vinylpyridine) quaternized by *n*-alkyl bromides of different chain length (x = 2, 4, 6, 8, 10) in methanol solution has been investigated by ^{13}C longitudinal relaxation at 25 MHz with some subsidiary T_1 and NOE measurements at 63 MHz. As in the case of poly(4-vinylpyridine) neutral or quaternized by HBr, the T_1's in the macromolecular chain and in the pyridyl rings have been interpreted by a quasi-isotropic segmental motion and a jump oscillation about the C(α)–C(4') axis, respectively, assuming a distribution of correlation times. The influence of the coulombic and steric effects on the internal motions of these polymers has been examined by varying the length of alkyl side chains and the degree of quaternization. Both of these parameters have a marked effect on the flexibility of the main chain and side chains but not on the axial motion of pyridyl rings. For the internal motion of alkyl side chains, we have considered three basic models of rotation about N–C or C–C bonds and some of their combinations: rotational diffusion (A), jump among three equivalent sites corresponding to the t, g^+, and g^- conformers (B), and same as (B) with t unequivalent to g^+, g^- (C). The consistency between the T_1 and NOE observed and computed for 25 and 63 MHz is achieved only for model C with $W(g^+ \rightleftarrows g^-) < W(t \rightarrow g^\pm) \leq 0.5W(g^\pm \rightarrow t)$.

The understanding of the dynamical behavior of hydrocarbon chains is important in many physicochemical problems, in particular those dealing with micellar solutions and membranes. In the last few years, several models have been proposed for the segmental motion of these chains,[1-8] but an unequivocal selection among them has not been achieved up to now. This problem prompted us to investigate the ^{13}C relaxation in poly(4-vinylpyridine), quaternized at different degree q by *n*-alkyl bromides of various chain length, the general formula of which is

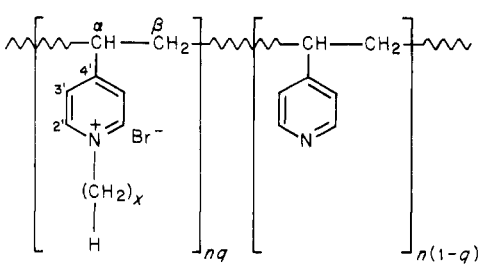

P4VPCx

We have previously interpreted the ^{13}C relaxation in alkyl side chains, either by a diffusional motion about C–C bonds[9] using a semiempirical treatment proposed by Levine et al.[1] or by random jumps of the methylene group among three unequivalent sites by means of the Monte-Carlo method.[7] These two different models lead to a satisfactory agreement with experiment at a single spectrometer frequency; we have reexamined this problem by means of a more general treatment[10] allowing for computation of the ^{13}C relaxation for several models of motion about the successive C–C bonds of an alkyl chain. In the present work, the ^{13}C longitudinal relaxation times and the ^{13}C {^1H} nuclear overhauser enhancement (NOE), computed at two different spectrometer frequencies (25 and 63 MHz), are compared to experimental data in order to select the most suitable model for the internal motions of the alkyl side chains.

We have also examined the influence of the degree of quaternization and of the length of alkyl side chains on the segmental motion of the macromolecular chain and on the rotational motion of pyridyl rings, assuming a dis-

0024-9297/79/2212-0775$01.00/0

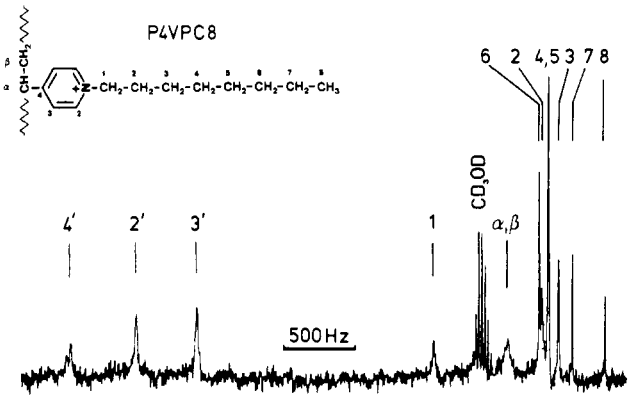

Figure 1. ^{13}C NMR spectrum of P4VPC8 (q = 100%) in CD_3OD at 300 K. Spectrometer frequency 25 MHz.

tribution of correlation times as in the case of poly(4-vinylpyridine) neutral (P4VP)[11] or quaternized by hydrobromic acid (P4VPD$^+$),[12] to which reference are made.

Experimental Section

The poly(4-vinyl-*N*-alkylpyridinium bromides) (P4VPCx) were obtained by reaction of P4VP with $CH_3(CH_2)_{x-1}Br$ in tetramethylene sulfone under nitrogen atmosphere with continuous stirring. The temperature and reaction time were adjusted according to the length of the alkyl bromide chain and the percentage of quaternization required. For instance, the 100% quaternization of P4VP by butyl bromide was obtained by dissolution of 1 g of P4VP in 100 mL of tetramethylene sulfone at 40 °C. Then an excess of butyl bromide was added and the solution was kept 1 week at 60 °C. The quaternized polymers were recovered by precipitation and washed in dry ethyl ether. The degree of quaternization in the course and after completion of the reaction was monitored by potentiometric titration and checked by ^1H and ^{13}C NMR (Figure 1).

Natural abundance ^{13}C NMR spectra were obtained with Varian XL 100 and Cameca TSN 250 spectrometers operating at 25.2 and 62.86 MHz, respectively. T_1 measurements were performed by the inversion recovery method (180°–τ–90° pulse sequences). The NOE were obtained from the ratios of the integrated intensities of resonance peaks under proton noise decoupling and without decoupling.

Theory

The calculations of ^{13}C relaxation rates have been made under the following assumptions: isotropic motion of the segments of the macromolecular chain with a distribution of the correlation times τ_R and rotational jumps of the pyridyl ring between two equivalent positions about the C(α)–C(4') axis (see ref 11 and 12). For the methylene or methyl groups of the alkyl side chain attached to the pyridyl ring, we have considered three models of rotation about the N–Cl and C–C bonds—(A) stochastic rotational diffusion, (B) random jumps among three equivalent sites, and (C) random jumps among three sites, two of them being equivalent.

The general expressions of the longitudinal and transverse relaxation rates and of the NOE for ^{13}C under noise decoupling of ^1H are[13]

$$T_1^{-1} = \frac{1}{20}K[J_0(\omega_C - \omega_H) + 3J_1(\omega_C) + 6J_2(\omega_H + \omega_C)] \quad (1)$$

$$T_2^{-1} = \frac{1}{40}K[4J_0(0) + J_0(\omega_C - \omega_H) + 3J_1(\omega_C) + 6J_1(\omega_H) + 6J_2(\omega_H + \omega_C)] \quad (2)$$

$$\mathrm{NOE} = 1 - \frac{\gamma_H}{\gamma_C}\frac{J_0(\omega_C - \omega_H) - 6J_2(\omega_C + \omega_H)}{J_0(\omega_C - \omega_H) + 3J_1(\omega_C) + 6J_2(\omega_C + \omega_H)} \quad (3)$$

with

$$K = \gamma_H^2\gamma_C^2\hbar^2 r_{CH}^{-6}$$

$\gamma_{H,C}$ and $\omega_{H,C}$ are the magnetogyric ratios and Larmor frequencies, respectively, and r_{CH} is the distance of ^{13}C to a directly attached proton.

For an exponential autocorrelation function, the spectral density is of the form:

$$J(\omega) = \frac{2\tau_c}{1 + \omega^2\tau_c^2} \quad (4)$$

which becomes

$$J(\omega) = \int_0^\infty \frac{2\tau_c G(\tau_c)}{1 + \omega^2\tau_c^2}\,d\tau_c \quad (5)$$

if there is a distribution of correlation times τ_c defined by the probability density function $G(\tau_c)$.

In the present study, we have used alternately the Fuoss–Kirkwood[14] distribution as in our preceding works[11,12] or the Cole–Cole[15] distribution. The relevant density functions are respectively

$$F(s) = \frac{\beta}{\pi}\frac{\cos(\beta[\pi/2])\cosh(\beta s)}{\cos^2(\beta[\pi/2]) + \sinh^2(\beta s)} \quad (6)$$

$$F(s) = \frac{1}{2\pi}\frac{\sin(\gamma\pi)}{\cosh(\gamma s) + \cos(\gamma\pi)} \quad (7)$$

with $s = \ln(\tau/\tau_A)$, τ_A being the center of the distribution at the logarithmic scale.

The widths of the distributions are defined by the parameters $0 < \beta \leq 1$ or $0 < \gamma \leq 1$. The Fuoss–Kirkwood and Cole–Cole distributions behave similarly and there is no shift of the T_1 minimum with respect to the case of a single correlation time ($\beta = \gamma = 1$). The correspondance between these two distributions may be found in ref 16; for a given value of the distribution width, β is slightly smaller than γ. The corresponding spectral densities are[16]

$$J(\omega) = \frac{2\beta\omega^{\beta-1}\tau_A^\beta}{1 + \omega^{2\beta}\tau_A^{2\beta}} \quad (8)$$

and

$$J(\omega) = \frac{1}{2\omega}\frac{\cos[(1-\gamma)(\pi/2)]}{\cosh[(\gamma\ln\omega\tau_A)] + \sin[(1-\gamma)(\pi/2)]} \quad (9)$$

The ^{13}C relaxation in the macromolecular chain is given by eq 1 through 9. For the pyridinyl ring, we have used the equation[11]

$$T_1^{-1} = \frac{3\hbar^2\gamma_C^2\gamma_H^2}{80}[\{\tfrac{2}{3}(1 - 3\cos^2\theta)^2 + (1 + \cos\alpha)\sin^2 2\theta + (1 + \cos 2\alpha)\sin^4\theta\}H(\tau_R) + \{(1 - \cos\alpha)\sin^2 2\theta + (1 - \cos 2\alpha)\sin^4\theta\}H(\tau_t)] \quad (10)$$

assuming for simplicity that the correlation time distribution is the same for τ_R and τ_t:

$$H(\tau) = \beta\tau^\beta\left\{\frac{(\omega_H - \omega_C)^{\beta-1}}{1 + (\omega_H - \omega_C)^{2\beta}\tau^{2\beta}} + \frac{3\omega_C^{\beta-1}}{1 + \omega_C^{2\beta}\tau^{2\beta}} + \frac{6(\omega_H + \omega_C)^{\beta-1}}{1 + (\omega_H + \omega_C)^{2\beta}\tau^{2\beta}}\right\} \quad (11)$$

θ is the angle between a ^{13}C–H bond and the C(α)–C(4') axis, α is the amplitude of the rotational jump, and $\tau_t = (\tau_R^{-1} + \tau_G^{-1})^{-1}$, τ_G being the correlation time for this motion.

Equation 10 which has been used already for the motion of the pyridyl ring in P4VP[11] and P4VPD$^+$[12] may be derived also from eq 1 and eq 14 and 19 given below.

For the ^{13}C relaxation in the alkyl side chains, the spectral densities, according to the model of motion about C–C of N–C(1) bonds, follow:

(a) The internal motion of the alkyl chain is entirely diffusional[1,5]

$$J_h(\omega) = \tfrac{2}{5} \sum_{a,b,\ldots,n} (d_{ab}^{(2)}(\beta_1))^2 (d_{be}^{(2)}(\beta_2))^2 \ldots (d_{no}^{2)}(\beta_N))^2 f(\tau_p) \quad (12)$$

with

$$\tau_p = (\tau_R^{-1} + a^2 D_1 + b^2 D_2 + \ldots + n^2 D_N)^{-1} \quad (13)$$

(b) There is a jump rotation about all bonds[10]

$$J_h(\omega) = \tfrac{2}{5} \sum_{\substack{a,b,\ldots,n \\ b',\ldots,n' \\ q_1,\ldots,q_N}} d_{ab}^{(2)}(\beta_1) d_{ab'}^{(2)}(\beta_1) \ldots d_{no}^{(2)}(\beta_N) d_{n'o}^{(2)} \times (\beta_N) e^{-i(n-n')\alpha_N} A_{1aa}(q_1) \ldots A_{Nnn'}(q_N) f(\tau_p) \quad (14)$$

with

$$\tau_p = (\tau_R^{-1} + \sum_{k=1}^{N} \lambda_{q_k,k})^{-1} \quad (15)$$

(c) There is jump rotation about all bonds, except the Lth bond about which diffusional rotation occurs:

$$J_h(\omega) = \tfrac{2}{5} \sum_{\substack{a,b,\ldots,n \\ b',\ldots,n' \\ q_1 \ldots q_{L-1} q_{L+1} \ldots q_N}} \delta_{ll'} d_{ab}^{(2)}(\beta_1) d_{ab'}^{(2)}(\beta_1) \ldots d_{no}^{(2)} \times (\beta_N) d_{n'o}^{(2)}(\beta_N) e^{-\alpha_N i(n-n')} A_{1aa}(q_1) \ldots A_{L-1,(l-1),(l'-1)}(q_{L-1}) \times A_{L+1,(l+1),(l'+1)}(q_{L+1}) \ldots A_{Nnn'}(q_N) f(\tau_p) \quad (16)$$

(where $\delta_{ll'}$ = Kroneker's symbol) with

$$\tau_p = (\tau_R^{-1} + l^2 D_L + \sum_{k=1}^{N}{}' \lambda_{q_k,k})^{-1} \quad (17)$$

$\sum'$ means that the summation should be made for all bonds except the Lth.

In eq 12, 14, and 16 $d^{(2)}$ denotes the Wigner reduced second-order matrix, D are the coefficients of rotational diffusion about the bonds, and $a, \ldots, n, b', \ldots, n'$ and $q_1, \ldots, q_N$ are indices running from −2 to +2 and 1 to 3, respectively. α_L and β_L are the polar and azimuthal angles of the Lth carbon–hydrogen bond in the coordinate system fixed to the Lth group with the Z axis parallel to C_{L-1}–C_L and the X axis perpendicular to this bond in the C_{L-1}, C_L, C_{L+1} plane. λ_{q_k} is an eigenvalue of the matrix of kinetic coefficients:

$$W_L = \begin{vmatrix} -2W_{1L} & W_{2L} & W_{2L} \\ W_{1L} & -(W_{2L} + W_{3L}) & W_{3L} \\ W_{1L} & W_{3L} & -(W_{2L} + W_{3L}) \end{vmatrix} \quad (18)$$

where $W_{1,2,3}$ are the jump rates among three sites, sites 2 and 3 being equivalent:

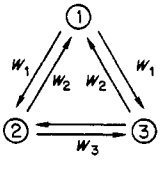

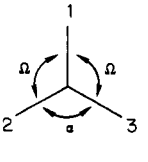

In eq 14 and 16, $A_{Lll'}(qL)$ are given by:

$$A_L^{(1)}{}_{ll'} = (2V_L + 1)^{-2}[1 + 2V_L \cos(l\Omega_L)] \times [1 + 2V_L \cos(l'\Omega_L)] e^{-i(l-l')\epsilon_L}$$

$$A_L^{(2)}{}_{ll'} = 2V_L(2V_L + 1)^{-2}[1 - \cos(l\Omega_L)][1 - \cos(l'\Omega_L)] e^{-i(l-l')\epsilon_L}$$

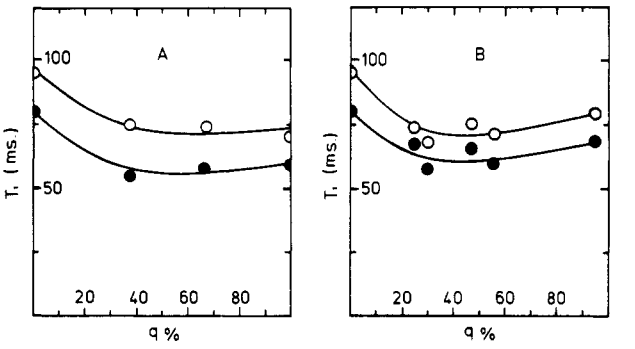

Figure 2. Dependence upon the degree of quaternization q of the T_1 relaxation time of the α carbon (●) and the pyridyl ring carbons (○) in P4VPC4 (A) and P4VPC8 (B) at 300 K ($\nu_{^{13}C}$ = 25 MHz).

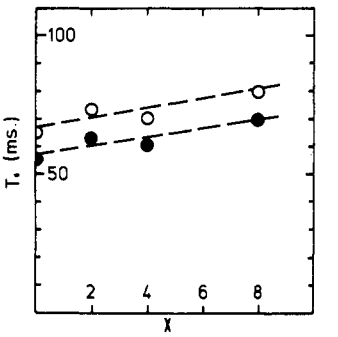

Figure 3. Dependence upon the alkyl side chain length of the T_1 relaxation time of the α carbon (●) and the pyridyl ring carbons (○) for a degree of quaternization $q \simeq 100\%$.

$$A_L^{(3)}{}_{ll'} = 2V_L(2V_L + 1)^{-1} \sin(l\Omega_L) \sin(l'\Omega_L) e^{-i(l-l')\epsilon_L} \quad (19)$$

where $V = W_1/W_2$, ϵ_L is the dihedral angle C_{L-2}, C_{L-1}, C_L, C_{L+1} defining the angular position of the site 1 about the C_{L-1}–C_L bond, and Ω_L is the rotational angle from site 1 to sites 2 or 3. In the expressions of $J_h(\omega)$, $f(\tau_p) = \tau_p(1 + \omega^2\tau_p^2)^{-1}$, which is averaged numerically in the cases where there is a distribution of τ_R. The derivations of eq 14 through 19 with some numerical applications are given in another article.[10]

Results and Discussion

The ^{13}C chemical shifts of the polymers under study, compared with those of P4VP and P4VPD$^+$, are given in Table I. It is seen that beyond C(6), the chemical shifts of terminal carbons of an alkyl chain, which do not experience the shielding effect of the pyridyl ring, become independent of its length. This point suggests, as in the case of paramagnetic complexes with long alkyl chains,[17] that the probability of occurrence of folded back conformations of these chains is very low.

The ^{13}C relaxation times T_1 given in Table II reveal the following main features:

There are no dramatic effects upon the degree of quaternization, of the relaxation times of the main chain, and of the pyridyl ring carbons, which are in the region of the shallow T_1 minimum. The T_1 dependence of these carbons upon q represented in Figure 2 suggests however an increase of the motional correlation time with the degree of quaternization.

The relaxation time of carbon 1 in the alkyl chain increases slightly with the degree of quaternization whereas the gradient of relaxation time along the side chains as well as the T_1 of terminal carbons decrease.

For a high degree of quaternization, the augmentation of the alkyl chain length brings about an increase of the T_1 of carbon α, which for $(\omega_H + \omega_C)^2\tau_R^2 > 1$ indicates that

Table I
^{13}C Chemical Shifts of P4VP, P4VPD$^+$, and P4VPCx, 1 M in Methanol Solution at 300 K (in ppm from Tetramethylsilane (Me_4Si))

		pyridyl ring			alkyl side chains									
polymers	$\alpha\beta$[a]	2'	3'	4'	1	2	3	4	5	6	7	8	9	10
P4VP	40.5	150.3	125.1	154.4										
P4VPD$^+$	42.5	143.2	128.5	166.1										
P4VPC2	41.8	145.2	128.8	164.1	57.7	16.7								
P4VPC4	41.8	145.6	128.7	164.0	62.3	33.8	20.6	13.9						
P4VPC6	42.6	145.5	128.4	164.0	62.2	32.1	26.7	32.1	23.4	14.3				
P4VPC8	42.1	145.6	128.6	164.4	62.4	32.0	27.3	30.3	30.1	32.8	23.6	14.4		
P4VPC10	42.3	145.4	128.5	164.6	62.4	32.2	27.3	30.5	30.5	30.5	30.5	32.9	23.6	14.4

[a] Partially superimposed lines.

Table II
^{13}C Longitudinal Relaxation Times in s at 25 MHz (T = 300 K) of P4VP, P4VPD$^+$, and P4VPCx in 1 M Methanol Solution[a]

				alkyl side chains									
polymers	q, %	$\alpha\beta$[b]	pyridyl ring	1	2	3	4	5	6	7	8	9	10
P4VP	0	0.080	0.095										
P4VPD$^+$	100	0.055	0.065										
P4VPC2	~100	0.063	0.073	0.108	0.70								
P4VPC4	37	0.054	0.075	0.057	0.22	0.58	1.28						
	66	0.058	0.074	0.080	0.21	0.50	1.21						
	~100	0.060	0.070	0.087	0.21	0.45	1.03						
P4VPC6	73	0.054	0.065	0.071	0.30[b]	0.41	1.00[b]	1.52	2.35				
P4VPC8	25	0.068	0.074	0.044	0.20	0.36	0.66[b]	0.82[b]	1.48	2.7	3.9		
	30	0.058	0.068	0.039	0.20	0.39	0.70[b]	0.80[b]	1.48	2.7	3.9		
	47	0.060	0.076	0.070	0.18	0.38	0.64[b]	0.64[b]	1.42	2.5	3.4		
	56	0.060	0.072	0.074	0.20	0.31	0.67[b]	0.67[b]	1.33	2.2	3.0		
	95	0.069	0.079	0.084	0.16	0.25	0.54[b]	0.54[b]	1.02	1.8	2.7		
P4VPC10	44	0.066	0.080	0.062	0.20	0.20	0.80[b]	0.80[b]	0.80[b]	0.80[b]	1.6	2.4	3.4

[a] Accuracy: ±10% for $T_1 < 0.1$ s and ±5% for $T_1 > 0.1$ s. [b] Overlapping resonances. In the case of $C_{\alpha\beta}$, it may be shown that the apparent T_1 is nearly that of C_α.[11,12]

Table III
(a) Parameters for the Calculations of the T^{-1} Dependence of C(α) Longitudinal Relaxation Times in the Macromolecular Chain

polymers[b]	β[a]	E_R, kcal mol^{-1}	$(\tau_R)_0$, s	T_{min}, K
P4VP (A)	0.75	5	2.1×10^{-15}	250
P4VPD$^+$ (B)	0.75	7	2.1×10^{-14}	286
P4VPC8 47% (C)	0.65	8	6.2×10^{-15}	297
P4VPC8 85% (D)	0.65	9	3.0×10^{-15}	317
P4VPC2 100% (E)	0.65	9	2.0×10^{-15}	308

(b) Parameters for the Calculation of the ^{13}C T_1's in the Pyridyl Ring, Taking E_G = 2 kcal mol^{-1}

polymers[b]	$(\tau_G)_0$, s	amplitude of jump[c]
P4VP (A)	9.65×10^{-12}	$74 \geqslant \alpha \geqslant 54$
P4VPD$^+$ (B)	1.39×10^{-11}	$62 \geqslant \alpha \geqslant 42$
P4VPC8 47% (C)	1.39×10^{-11}	$62 \geqslant \alpha \geqslant 42$
P4VPC8 95% (D)	9.65×10^{-12}	$58 \geqslant \alpha \geqslant 38$
P4VPC2 100% (E)	9.65×10^{-12}	$58 \geqslant \alpha \geqslant 38$

[a] Parameter of the Fuoss-Kirkwood distribution. [b] See Figure 4. [c] Amplitude of jump about C(α)-C(4') for $2.7 \leqslant 10^3/T \leqslant 3.7$.

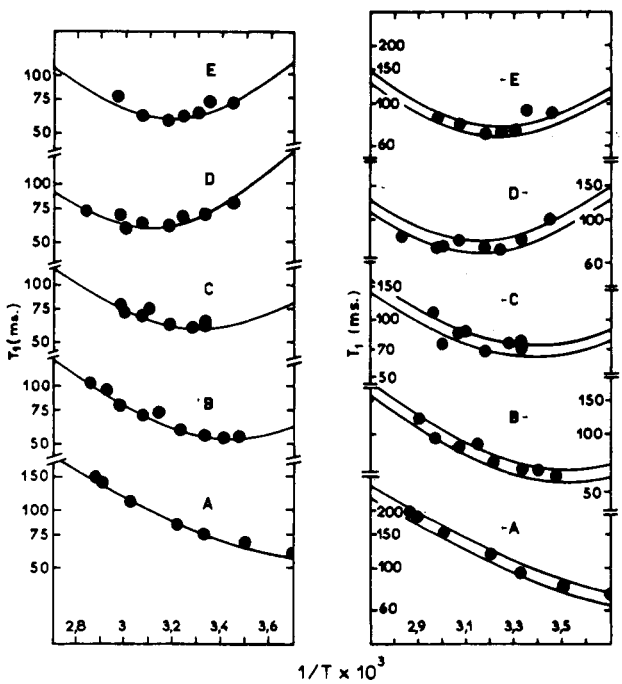

Figure 4. Left: Temperature dependence of the T_1 relaxation time of α carbon in (A) P4VP, (B) P4VPD$^+$, (C) P4VPC8 (q = 45%), (D) P4VPC8 (q = 95%), and (E) P4VPC2 (q = 100%). The solid lines are computed with the parameters of Table IIIa. Right: Temperature dependence of the T_1 of pyridyl ring carbons in the same polymers as above. For each case, the upper curve is calculated for C(2,6) and the lower for C(3,5); the relevant parameters are given in Table IIIb.

the macromolecular chain becomes more rigid (Figure 3). We shall now consider successively the ^{13}C relaxation in the main chain, in the pyridyl ring, and in alkyl side chains in terms of internal motions.

(a) Segmental Motions in the Macromolecular Chain. The temperature dependence of the T_1 of carbon-13 in the main chain has been investigated for P4VPC2 (q = 100%) and P4VPC8 (q = 47 and 95%) and compared with our previous data on P4VP and P4VPD$^+$ for a spectrometer with frequency of 25 MHz. The $T_1 = f(T^{-1})$ curves have been simulated assuming a quasi-isotropic segmental motion and a Fuoss-Kirkwood distribution of correlation times, with $\tau_R = (\tau_R)_0 \exp(E_R/RT)$ $[(\tau_R)_0 = 5 \times 10^{-9} \exp(-E_R/RT_{min})]$ at 25 MHz, T_{min} being

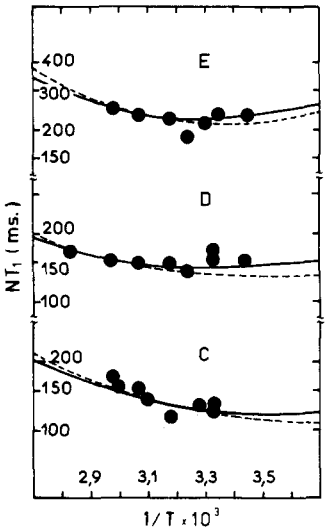

Figure 5. Temperature dependence of the T_1 relaxation time of carbon 1 of the alkyl side chains: (C) P4VPC8 (q = 47%), (D) P4VPC8 (q = 95%), (E) P4VPC2 (q = 100%). The solid lines are calculated with E_I = 1 kcal mol^{-1} and $(\tau_I)_0 = 1.8 \times 10^{-11}$, 1.3×10^{-11}, and 3.7×10^{-12} s for polymers C, D, and E, respectively. Dotted lines: E_I = 2 kcal mol^{-1}, $(\tau_I)_0 = 3.7 \times 10^{-12}$, 2.5×10^{-12}, and 7.7×10^{-13} s for C, D, and E, respectively.

the temperature corresponding to the minimum of T_1 vs. T^{-1} (Figure 4). The parameters used in these simulations are given in Table III. It is seen that the presence of alkyl side chains brings about a broadening of the correlation time distribution. The rigidification of the macromolecular chain under the conjugated effects of coulombic and steric interactions between side chains is evidenced by a significant increase of the activation energy upon protonation and alkylation and even more clearly by the shift of the T_1 minima toward higher temperatures. These two contributions may be separated by comparison of the data from P4VP and P4VPD$^+$ on one hand and P4VPC2 and P4VPC8 on the other. It appears that the coulombic interaction has a predominant effect on the dynamical behavior of the macromolecular chain.

(b) Motion of the Pyridyl Rings. The model of a jump rotational motion of the pyridyl ring about the C(α)–C(4′) axis which has provided a satisfactory interpretation of the ^{13}C and ^{1}H relaxations in P4VP and P4VPD$^+$[11,12] has been applied to the polymers under study, assuming a linear dependence of the rotational angle α upon T^{-1} and the correlation time distribution to be the same for τ_R and $\tau_t = (\tau_R^{-1} + \tau_G^{-1})^{-1}$ with $\tau_G = (\tau_G)_0 \cdot \exp(E_G/RT)$. The $T_1 = f(T^{-1})$ curves have been computed for P4VP and quaternized polymers with a common value E_G = 2 kcal mol^{-1} (Figure 4). In these calculations, the slight inequivalence of C(2,6) and C(3,5) was taken into account with C(2)–H(2) = 1.11 Å, θ = 57°, and C(3)–H(3) = 1.08 Å, θ = 60°.[18]

It is shown in Table III that the preexponential factor $(\tau_G)_0$ remains nearly unchanged upon protonation of the pyridyl ring or quaternization by an alkyl chain, whereas the rotational amplitude α about the C(α)–C(4′) axis is slightly restricted. The present work indicates therefore that the quaternization of P4VP by hydrogen or alkyl bromides has only a weak influence on the axial motion of the pyridyl ring.

(c) Rotation of the Alkyl Groups about the N–C(1) Bond. Before discussing the segmental motion of the alkyl side chains, we shall consider the relaxation of the first carbon (C(1)) attached to the nitrogen which is expected to be the most dependent upon the degree of quaternization. For the simulation of the temperature dependence

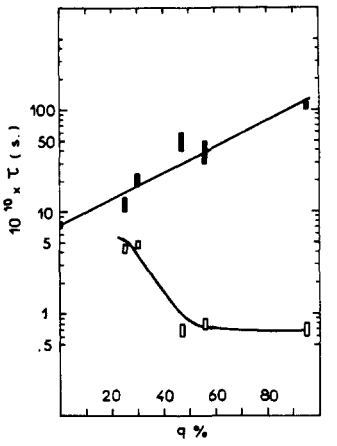

Figure 6. Dependence of τ_A (■) and τ_I (□) at 300 K upon the degree of quaternization of P4VP by octyl bromide at 300 K.

Table IV

(a) Experimental T_1 and NOE at 25 and 63 MHz for P4VPC4 in Methanol Solution (T = 300 K)

	C(α)	C(1)	C(2)	C(3)	C(4)
P4VPC4 (q = 37%)					
25 MHz NT_1, s	0.054	0.114	0.44	1.16	3.84
NOE	1.9	1.8	2.2	2.5	2.7
63 MHz NT_1, s	0.12	0.26	0.64	1.50	4.8
NOE	1.8	2.0	2.6	2.6	2.6
P4VPC4 (q = 100%)					
25 MHz NT_1, s	0.060	0.174	0.42	0.9	3.1
NOE	1.6	1.8	2.3	2.5	2.6
63 MHz NT_1, s	0.16	0.34	0.76	1.5	5.4
NOE	1.6	2.0	2.7	2.8	2.9

(b) T_1 and NOE Calculated for the α Carbon of the Main Chain

	$\nu_{^{13}C}$, MHz	T_1	NOE
P4VPC4 (q = 37%)			
γ = 0.8	25	0.058	1.87
$\tau_A = 2 \times 10^{-9}$ s	63	0.130	1.51
P4VPC4 (q = 100%)			
γ = 0.75	25	0.059	1.46
$\tau_A = 7 \times 10^{-9}$ s	63	0.190	1.34

of the T_1 of this carbon, we have chosen the simplest model of diffusional rotation of the first methylene group. This model requires indeed a limited number of readily adjustable parameters, namely τ_R, the distribution parameter, and the rotation correlation time about N–C(1), $\tau_I = (6D_1)^{-1}$, the two former being provided by the C(α) relaxation. The longitudinal relaxation of C(1) in the case of a diffusional rotation is[13]

$$(2T_1)^{-1} = \frac{\hbar^2\gamma_C^2\gamma_H^2}{40r_{CH}^6}[(3\cos^2\theta - 1)^2 H(\tau_R) + 3\sin^2 2\theta(H(\tau_D)) + 3\sin^4\theta(H(\tau_E))] \quad (20)$$

where

$$\tau_D = (\tau_R^{-1} + (6\tau_I)^{-1})^{-1},\ \tau_E = (\tau_R^{-1} + 2(3\tau_I)^{-1})^{-1}$$

$H(\tau)$ being given by eq 11. θ is the angle between C(1)–H and the C(4′)–N axis. The $T_1 = f(T^{-1})$ curves have been computed with an activation energy E_I = 1.5 ± 0.5 kcal mol^{-1} and β = 0.65. Figure 5 shows that the values of T_1 at the minimum of curves are in the order P4VPC2 (q = 100%) > P4VPC8 (q = 95%) > P4VPC8 (q = 47%). While the T_1 minima occur at nearly the same temperature for P4VPC8 (q = 95%) and P4VPC2 (q = 100%), the minimum is shifted toward lower temperature for P4VPC8 (q = 47%). This behavior is a first indication that the

Table V
^{13}C Relaxation in Butyl Side Chains[a]

P4VPC4 (q = 37%)

	N-C(1)	C(1)-C(2)	C(2)-C(3)	C(3)-C(4)
D, s^{-1}	9.0×10^8	5.1×10^9	8.2×10^9	3.7×10^{10} (a)
W, s^{-1}				3.0×10^{10} (b)
	C(1)	C(2)	C(3)	C(4)
25 MHz NT_1, s	0.12	0.43	1.13	3.72 (a)
				3.84 (b)
NOE	2.59	2.82	2.94	2.97 (a, b)
63 MHz NT_1, s	0.17	0.50	1.18	3.78 (a, b)
NOE	2.31	2.74	2.92	2.96 (a, b)

P4VPC4 (q = 100%)

	N-C(1)	C(1)-C(2)	C(2)-C(3)	C(3)-C(4)
D, s^{-1}	2.3×10^9	3.0×10^9	5.0×10^9	3.5×10^{10} (a)
W, s^{-1}				3.0×10^{10} (b)
	C(1)	C(2)	C(3)	C(4)
25 MHz NT_1, s	0.18	0.42	0.88	3.31 (a)
				3.33 (b)
NOE	2.41	2.83	2.95	2.97 (a, b)
63 MHz NT_1, s	0.27	0.47	0.91	3.36 (a)
				3.38 (b)
NOE	2.49	2.83	2.94	2.97 (a, b)

[a] Models A A A A (a) and A A A B (b).

Table VI
^{13}C Relaxation in Butyl Side Chains[a]

P4VPC4 (q = 37%)

	N-C(1)	C(1)-C(2)	C(2)-C(3)	C(3)-C(4)
(a) W, s^{-1}	7.0×10^8	4.0×10^9	5.0×10^9	3.0×10^{10}
(b) D, s^{-1}	9.0×10^8			
W, s^{-1}		4.0×10^9	6.0×10^9	3.0×10^{10}
	C(1)	C(2)	C(3)	C(4)
25 MHz (a) NT_1, s	0.12	0.45	1.09	3.74
NOE	2.66	2.85	2.95	2.98
(b) NT_1, s	0.12	0.44	1.18	3.91
NOE	2.59	2.82	2.94	2.97
63 MHz (a) NT_1, s	0.16	0.51	1.13	3.79
NOE	2.42	2.78	2.94	2.97
(b) NT_1, s	0.17	0.51	1.23	3.98
NOE	2.31	2.76	2.92	2.97

P4VPC4 (q = 100%)

	N-C(1)	C(1)-C(2)	C(2)-C(3)	C(3)-C(4)
(a) W, s^{-1}	1.6×10^9	2.2×10^9	4.0×10^9	2.5×10^{10}
(b) D, s^{-1}	2.3×10^9			
W, s^{-1}		2.5×10^9	4.0×10^9	3.0×10^{10}
	C(1)	C(2)	C(3)	C(4)
25 MHz (a) NT_1, s	0.18	0.44	0.88	3.06
NOE	2.44	2.84	2.95	2.98
(b) NT_1, s	0.18	0.43	0.94	3.46
NOE	2.41	2.83	2.95	2.97
63 MHz (a) NT_1 s	0.25	0.48	0.90	3.09
NOE	2.62	2.89	2.96	2.98
(b) NT_1, s	0.27	0.48	0.97	3.50
NOE	2.49	2.86	2.96	2.98

[a] Models B B B B (a) and A B B B (b).

rotational freedom about N–C(1) decreases with the chain length and increases with the degree of quaternization (see for instance in ref 13 the discussion about the combined effects of τ_R and τ_I on the ^{13}C relaxation). The influence of the degree of quaternization is more explicitly demonstrated on the example of P4VPC8 where τ_R and τ_I are plotted as a function of the degree of quaternization (Figure 6). While the correlation time τ_R of the segmental motion of the main chain increases steadily with q, there is a sharp decrease of τ_I between q = 25% and q = 60%. A tentative explanation of these results is that the mutual repulsion between the positively charged pyridyl rings leaves a free volume available for the rotation of alkyl chains. A similar effect is observed in the case of P4VPC4 (Table II). On the other hand, an increase of the alkyl chain length reduces the rotational freedom about N–C(1) as shown by a decrease of T_1 (Table II).

(d) Internal Motion of the Alkyl Side Chains. To

Table VII
Experimental and Calculated T_1 of P4VPC8 in CD_3OD (300 K, $\nu_{^{13}C}$ = 25 MHz)

			P4VPC8 (q = 25%)				
main chain	$\tau_R = 1.5 \times 10^{-9}$ s, $\gamma = 0.8$						
side chain		N-C(1)	C(1)-C(2)	C(2)-C(3)	C(3)-C(4)	C(4)-C(5)	C(5)-C(6)
D, s^{-1}		4.0×10^8	5.0×10^9	5.0×10^9	5.0×10^9	5.0×10^9	1.0×10^{10}
	C(α)	C(1)	C(2)	C(3)	C(4)	C(5)	C(6)
T_1, s exptl	0.063	0.088	0.40	0.72	1.32	1.64	2.91
T_1, s calcd	0.062	0.090	0.37	0.83	1.36	1.86	2.85
			P4VPC8 (q = 100%)				
main chain	$\tau_R = 1.0 \times 10^{-8}$ s, $\gamma = 0.75$						
side chain		N-C(1)	C(1)-C(2)	C(2)-C(3)	C(3)-C(4)	C(4)-C(5)	C(5)-C(6)
D, s^{-1}		2.2×10^9	2.5×10^9	2.5×10^9	2.5×10^9	2.5×10^9	1.0×10^{10}
	C(α)	C(1)	C(2)	C(3)	C(4)	C(5)	C(6)
T_1, s exptl	0.060	0.17	0.32	0.50	1.08	1.08	2.04
T_1, s calcd	0.064	0.175	0.37	0.62	0.86	1.11	2.04

Table VIII
^{13}C Relaxation in Butyl Side Chains[a]

		P4VPC4 (q = 37%)		
	N-C(1)	C(1)-C(2)	C(2)-C(3)	C(3)-C(4)
D, s^{-1}	9.0×10^8			
(a) $W_2 = 2W_1$ ($W_3 = 0$)		1.0×10^{10}	1.4×10^{10}	
W				3.5×10^{10}
(b) $W_2 = 2W_1$ ($W_3 = 0$)	1.8×10^9	1.0×10^{10}	1.0×10^{10}	
W				3.2×10^{10}
	C(1)	C(2)	C(3)	C(4)
25 MHz (a) NT_1, s	0.12	0.44	1.13	3.8
NOE	2.59	2.86	2.89	2.94
(b) NT_1, s	0.12	0.45	1.06	3.7
NOE	2.53	2.81	2.85	2.95
63 MHz (a) NT_1, s	0.17	0.51	1.26	3.9
NOE	2.31	2.71	2.83	2.88
(b) NT_1, s	0.18	0.53	1.15	3.84
NOE	2.38	2.74	2.88	2.94
		P4VPC4 (q = 100%)		
	N-C(1)	C(1)-C(2)	C(2)-C(3)	C(3)-C(4)
D, s^{-1}	2.3×10^9			
(a) $W_2 = 2W_1$ ($W_3 = 0$)		5.0×10^9	1.0×10^{10}	
W				2.5×10^{10}
(b) $W_2 = 2W_1$ ($W_3 = 0$)	4.0×10^9	4.0×10^9	1.2×10^{10}	
W				2.5×10^{10}
	C(1)	C(2)	C(3)	C(4)
25 MHz (a) NT_1, s	0.18	0.43	0.87	3.1
NOE	2.41	2.91	2.85	2.97
(b) NT_1, s	0.17	0.42	0.90	3.24
NOE	2.20	2.80	2.83	2.95
63 MHz (a) NT_1, s	0.27	0.46	0.95	3.2
NOE	2.49	2.87	2.90	2.95
(b) NT_1, s	0.28	0.47	0.98	3.31
NOE	2.48	2.86	2.91	2.97

[a] Models A C C B (a) and C C C B (b) with $W_1(t \rightarrow g) = 0.5W_2(g \rightarrow t)$; $W_3(g^+ \rightleftarrows g^-) = 0$.

interpret the ^{13}C longitudinal relaxation and the NOE in alkyl side chains at 25 and 63 MHz we have considered three basic models of rotation of the methylene groups, taking into account the distribution of correlation times in the macromolecular chain: (A) stochastic rotational diffusion; (B) random jump among three equivalent sites corresponding to the trans (t) and gauche (g^+, g^-) rotamers about C–C bonds; and (C) random jump among three sites, two of them being equivalent (gauche rotamers). The validity of these models and of some of their combinations has been examined on the P4VPC4 with q = 37 and 100%. The different assumptions for the internal motions of the butyl chain in these polymers are summarized in Chart I.

The parameters used in the calculation of the ^{13}C relaxation in the macromolecular chain of the P4VPC4 at 300 K are given in Table IV together with the relevant experimental data.

The parameter γ of the Cole–Cole distribution has been taken equivalent to the parameter β of the Fuoss–Kirkwood distribution obtained from the simulation of the temperature dependence of the ^{13}C T_1 relaxation times of other quaternized polymers (Table IV). The kinetic parameters for the motion of the methylene and methyl groups were obtained by adjusting the T_1 computed for 25 MHz to the experimental values. The validities of assumptions I through VI were checked from a further agreement between the computed and experimental T_1 obtained at 63 MHz and also from the NOE at both frequencies, although the determination of the latter is less accurate than for the relaxation times.

At a single spectrometer frequency of 25 MHz, the T_1 computed for assumptions I through IV are readily fitted to experimental data by adjusting the diffusion coefficient or the jump rate W among three equivalent sites about

Table IX
^{13}C Relaxation in Butyl Side Chains[a]

P4VPC4 (q = 37%)

	N-C(1)	C(1)-C(2)	C(2)-C(3)	C(3)-C(4)
(a) D, s^{-1}	9.0×10^8			
W_1, s^{-1}		5.0×10^9	5.0×10^9	
W_2, s^{-1}		1.0×10^{10}	1.0×10^{10}	
W_3, s^{-1}		1.0×10^9	5.0×10^9	
W, s^{-1}				3.5×10^{10}
(b) W_1, s^{-1}	2.0×10^9	4.2×10^9	5.0×10^9	
W_2, s^{-1}	1.0×10^{10}	1.0×10^{10}	1.0×10^{10}	
W_3, s^{-1}	1.0×10^9	3.0×10^9	5.0×10^9	
W, s^{-1}				3.0×10^{10}

	C(1)	C(2)	C(3)	C(4)
25 MHz (a) NT_1, s	0.12	0.45	1.15	3.86
NOE	2.59	2.85	2.83	2.93
(b) NT_1, s	0.12	0.47	1.23	4.01
NOE	1.99	2.33	2.68	2.85
63 MHz (a) NT_1, s	0.17	0.53	1.29	4.12
NOE	2.31	2.72	2.83	2.88
(b) NT_1, s	0.24	0.71	1.46	4.32
NOE	1.83	2.42	2.78	2.90

P4VPC4 (q = 100%)

	N-C(1)	C(1)-C(2)	C(2)-C(3)	C(3)-C(4)
(a) D, s^{-1}	2.3×10^9			
W_1, s^{-1}		2.7×10^9	5.0×10^9	
W_2, s^{-1}		1.0×10^{10}	1.0×10^{10}	
W_3, s^{-1}		1.0×10^9	3.0×10^9	
W, s^{-1}				2.4×10^{10}
(b) W_1, s^{-1}	3.0×10^9	3.0×10^9	5.0×10^9	
W_2, s^{-1}	1.0×10^{10}	1.0×10^{10}	1.0×10^{10}	
W_3, s^{-1}	1.0×10^9	1.0×10^9	2.0×10^9	
W, s^{-1}				2.5×10^{10}

	C(1)	C(2)	C(3)	C(4)
25 MHz (a) NT_1, s	0.18	0.43	0.90	3.15
NOE	2.41	2.53	2.62	2.97
(b) NT_1, s	0.16	0.50	1.01	3.63
NOE	1.72	2.21	2.51	2.86
63 MHz (a) NT_1, s	0.27	0.48	1.11	3.27
NOE	2.49	2.78	2.79	2.93
(b) NT_1, s	0.39	0.78	1.30	3.86
NOE	1.99	2.58	2.78	2.94

[a] Models A C C B (a) and C C C B (b) with $W_3(g^+ \rightleftarrows g^-) < W_1(t \rightarrow g) \leq 0.5W_2(g \rightarrow t)$.

Chart I

	N-C(1)	C(1)-C(2)	C(2)-C(3)	C(3)-C(4)
		Table V		
I	A	A	A	A
II	A	A	A	B
		Table VI		
III	A	B	B	B
IV	B	B	B	B
		Tables VIII and IX		
V	A	C	C	B
VI	C	C	C	B

N-C(1) and C-C bonds (Tables V-VII). These assumptions do not hold when the data computed for 63 MHz are compared to the experimental values. Assuming however that the diffusion model I gives a semiquantitative picture of the segmental mobility along an alkyl chain fixed to a macromolecule, we have computed the T_1 at 25 MHz for carbons 1 through 6 in P4VPC8 with q = 25 and 95% (Table VII). The most striking feature is the absence of a gradient of rotational diffusion between C(2) and C(4) or C(5) for q = 25 and 95%, respectively.

The models V and VI which require much longer computation times have been limited to the butyl chain. For the jump rotation among three unequivalent sites (model C) we have assumed either that $W_1(t \rightarrow g)/W_2(g \rightarrow t) = 0.5$ with $W_3(g^+ \rightleftarrows g^-) = 0$ as for our previous computations of T_1 by the Monte-Carlo method[7] or that $W_3 < W_1 \leq 0.5W_2$. Both assumptions seem convenient for models V and VI at 25 MHz (Tables VIII and IX); however, the best consistency between the experimental and computed T_1 and NOE data at 25 and 63 MHz is only achieved for model VI with $W_3 < W_1 \leq 0.5W_2$. A study in progress on the ^{13}C relaxation in n-alkylamines coordinated to paramagnetic ions[19] leads to similar conclusions. It appears in particular that the augmentation of the rotational freedom from the fixed to the free chain end is more conveniently represented by an increase of the W_1/W_2 ratio than by a variation of the absolute jump rates, at least if W_1 and W_2 are larger than τ_R^{-1}.

References and Notes

(1) Y. K. Levine, P. Partington, and G. C. K. Roberts, *Mol. Phys.*, **25**, 493 (1973).
(2) Y. K. Levine, N. J. M. Birdsdall, A. G. Lee, J. C. Metcalfe, P. Partington, and G. C. K. Roberts, *J. Chem. Phys.*, **60**, 2890 (1974).
(3) R. E. London and J. Avitabile, *J. Chem. Phys.*, **65**, 2443 (1976).
(4) R. E. London and J. Avitabile, *J. Am. Chem. Soc.*, **99**, 7765 (1977).
(5) G. C. Levy, D. E. Axelson, R. Schwartz, and J. Hochmann, *J. Am. Chem. Soc.*, **100**, 410 (1978).

(6) R. J. Wittebort and A. Szabo, *J. Chem. Phys.*, **69**, 1722 (1978).
(7) T. Yasukawa, D. Ghesquiere, and C. Chachaty, *Chem. Phys. Lett.*, **45**, 279 (1977).
(8) A. Tsutsumi, *Mol. Phys.*, **37**, 111 (1979).
(9) D. Ghesquiere, C. Chachaty, Buu Ban, and C. Loucheux, *Makromol. Chem.*, **177**, 1601 (1976).
(10) A. Tsutsumi and C. Chachaty, *Macromolecules*, in press.
(11) D. Ghesquiere, Buu Ban, and C. Chachaty, *Macromolecules*, **10**, 743 (1977).
(12) D. Ghesquiere and C. Chachaty, *Macromolecules*, **11**, 246 (1978).
(13) D. Doddrell, V. Glushko, and A. Allerhand, *J. Chem. Phys.*, **56**, 3683 (1972).
(14) R. M. Fuoss and J. G. Kirkwood, *J. Am. Chem. Soc.*, **63**, 385 (1941).
(15) K. S. Cole and R. H. Cole, *J. Chem. Phys.*, **9**, 329 (1941).
(16) T. M. Connor, *Trans. Faraday Soc.*, **60**, 1574 (1964).
(17) T. Yasukawa and C. Chachaty, *Chem. Phys. Lett.*, **43**, 565 (1976).
(18) C. Rerat, *Acta Crystallogr.*, **15**, 427 (1962).
(19) A. Tsutsumi, J. P. Quaegebeur, and C. Chachaty, *Mol. Phys.*, in press.

Ethylene–Propylene Copolymers and Mechanism of Steric Control

A. Zambelli,* M. C. Sacchi, and P. Locatelli

Istituto di Chimica delle Macromolecole del C.N.R., 20133 Milano, Italy.
Received March 5, 1979

ABSTRACT: The high-resolution ^{13}C NMR spectra of a sample of isotactic ^{13}C-enriched ethylene–propylene copolymer and of 2,4,8,10-tetramethylundecane are compared. The previous conclusions concerning the unique stereochemical placement of isolated ethylene units in isotactic copolymers and the mechanism of the isotactic steric control are confirmed.

In a recent paper,[1] conformational differences among the various propylene stereosequences were utilized for predicting the ^{13}C NMR chemical shifts of the carbons (labeled 5, 6, 7 in I below) of the ethylene–propylene copolymers containing isolated ethylene units flanked by long head-to-tail propylene sequences:

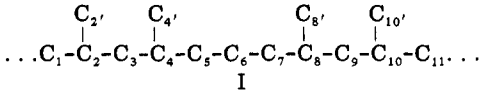

I

The predicted shifts[1] were in agreement with those previously measured in model compounds[2] except for the influence of the relative configuration of C_4 and C_8 on the chemical shift of the C_5–C_7 pair and of C_6. For instance, according to ref 1, the shift difference between the methylene carbons concerned in the stereosequences here drawn in Fisher projection

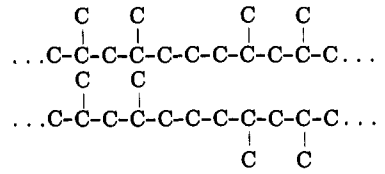

(called $T^mmE^mmT^m$ and $T^mmE^rmT^m$ in ref 1 and ++,++ and ++,−− in ref 2) should be undetectable. On the contrary, according to ref 2, at least the difference between the chemical shifts of the C_5–C_7 pairs would be detected.

The argument is by no means irrelevant because it involves the conclusions, exactly opposite in ref 1 and 2, concerning the suitability of the ^{13}C NMR analysis of ethylene–propylene copolymers in order to establish the mechanism of the steric control in isotactic specific polymerization of α-olefins.

On this subject, it may be of some use to compare the spectra of 2,4,8,10-tetramethylundecane (TMU) and of a copolymer of 90% enriched $^{13}CH_2{=}CH_2$ (0.05 mol %) with natural abundance propylene (99.95 mol %), prepared in the presence of the highly isotactic-specific catalyst system ARA $TiCl_3$–$Al(C_2H_5)_2I$[3] (Figure 1A,B).

TMU has been chosen for comparison because it comprises only two asymmetric carbons, so that splitting of the resonance of the C_5–C_7 pair can arise only from the relative configuration of C_4 and C_8 and because it is a more realistic model of the copolymer than 3,7-dimethylnonane (DMN), reported in a previous pioneering paper.[4]

In Figure 1A it may be observed that only one unsplit resonance is observed for C_6 of TMU while two resonances ($\Delta\nu$ = 0.04 ppm) are observed for the C_5–C_7 pairs in meso and racemic TMU (see expanded spectra).

In the spectrum of the copolymer, the completely isotactic arrangement of the propylene units can be appreciated (methyl, methylene, and methine resonances at 19.7_9,44.5_9, and 27.0_0 ppm, respectively). In addition, only two sharp resonances of the same intensity and of the same half-height width are observed for the C_5–C_7 pair and for C_6 (the equal intensity is due to the selective enrichment of $^{13}CH_2{=}CH_2$).

The resonances observed in the spectrum of the copolymer for C_5–C_7 and C_6 are wider than those observed in the spectrum of TMU, but a splitting such as that observed for the C_5–C_7 pair in meso and racemic TMU should still be easily detected also in the copolymer, at least as a broadening of the resonance at 35.9_2 ppm in comparison with that at $22,5_0$. Such a splitting has never been observed by us even by artificially reducing the width of the signals by multiplication of the FID with a suitable triangular function or by Sanders and Komoroski, who previously observed isotactic ethylene–propylene copolymers at higher magnetic field.[5]

In addition, an increasing splitting has been observed between the resonances of C_4–C_6 pairs in meso and racemic DMN ($\nu_r - \nu_m$ = −0.03 ppm)[6] and the resonances in C_5–C_7 pairs in meso and racemic TMU ($\nu_r - \nu_m$ = +0.04 ppm).

Therefore, we expect that in the spectrum of the isotactic copolymer, provided that more than one unique configurational stereosequence, including substituted

0024-9297/79/2212-0783$01.00/0